

SPORE Entry, Descent and Landing

David A. Spencer¹, Nicole Bauer², Jessica Juneau², Allison Willingham², Amit Mandalia² and Jenny Kelly³
Georgia Institute of Technology, Atlanta, GA, 30332

Justin McClellan⁴
Aurora Flight Sciences, Cambridge, MA, 02142

The Small Probes for Orbital Return of Experiments (SPORE) flight system is designed to perform atmospheric entry, descent and landing (EDL) in order to return small payloads from an Earth orbit to the ground for recovery and laboratory analysis. One such capability that the SPORE system will provide is in-situ flight test data of various Thermal Protection Systems (TPS), to be used for comparison to ground-based Arcjet test data and analyses. The following paper summarizes the current design of the SPORE TPS testbed mission and the various analyses and trade studies performed in order to converge on an entry system design. In particular, the driving EDL requirements are discussed as well as the nominal entry state (with dispersions) and trajectory design. An overall description of the entry vehicle packaging is included, with additional discussion of the parachute selection and deployment criteria. In addition, the entry vehicle thermal soak-back characterization is described as well as the re-entry stability analysis. The current mass budget for the entry system is included.

Nomenclature

ACS	= Attitude Control System
D_{max}	= Maximum entry vehicle diameter (m)
DOF	= Degree of Freedom
ϵ	= Surface emissivity
EDL	= Entry, Descent, and Landing
FIAT	= Fully Implicit Ablation and Thermal Response program
FPA	= Flight Path Angle
GPS	= Global Positioning System
GTO	= Geosynchronous Transfer Orbit
ISS	= International Space Station
LEO	= Low Earth Orbit
PD	= Proportional Derivative
PICA	= Phenolic Impregnated Carbon Ablator (TPS)
POST	= Program to Optimize Simulated Trajectories
q_{conv}	= Stagnation point convective heat flux (W/cm ²)
q_{rad}	= Stagnation point radiative heat flux (W/cm ²)
q_{rerad}	= Re-radiated heat flux (W/cm ²)
SPORE	= Small Probes for Orbital Return of Experiments
σ	= Stefan-Boltzmann constant (5.67e-8 W/cm ² /K ⁴)
TPS	= Thermal Protection System
T_{surf}	= TPS surface wall temperature (K)
UTTR	= Utah Test and Training Range

¹ Professor of the Practice, School of Aerospace Engineering, Mail Stop 0150, AIAA Associate Fellow.

² Graduate Research Assistant, School of Aerospace Engineering, Mail Stop 0150, AIAA Student Member.

³ Research Engineer, School of Aerospace Engineering, Mail Stop 0150, AIAA Member.

⁴ Aerospace Engineer, Research & Development Center, 1 Broadway 12th Floor, Cambridge, MA 02210

I. Introduction

THE Small Probes for Orbital Return of Experiments (SPORE) flight system architecture provides a scalable, modular approach to the return and recovery of multi-purpose probes from orbit. Capable of accommodating payload volumes ranging from the 1-unit (1U) dimensions of 10x10x10 cm to 2U and 4U payloads, SPORE is targeted to carry flight experiments related to thermal protection system (TPS) performance validation, biological science, and materials science missions. SPORE is also designed to accommodate the return of small payloads from the International Space Station (ISS). The following paper will focus on the design of the entry, descent, and landing sequence for the TPS flight-experiment scenario, with both return from low-Earth (LEO) and geosynchronous transfer (GTO) initial orbits.

As a testbed for thermal protection system validation, SPORE will provide in-flight characterization of instrumented heat shields using experimental TPS materials. The payload within the SPORE entry vehicle will consist of a data recording system that will enable the post-flight evaluation of the heat shield performance. The size of the entry probe will permit a 1:1 geometric similitude between the ground test and flight article, allowing the same probe to be tested both on the ground and in-flight at full scale. Demonstration of TPS technologies on an affordable flight platform will advance the technology readiness levels of new TPS concepts as well as evolved applications of heritage designs.

SPORE EDL is designed to meet thermal control and g-level requirements to maintain payload health and safety. Because the desired on-orbit environment for different payloads varies dramatically, the SPORE architecture is designed to accommodate re-entry from orbits ranging from low-Earth orbit (including ISS return) and GTO. Landing sites at the Utah Test & Training Range and the Woomera Test Range in South Australia are targeted.

II. Entry Descent and Landing Sequence of Events

The SPORE entry vehicle will be deployed following a de-orbit maneuver performed by the service module. The deployment attitude is selected to target zero angle-of-attack at entry with respect to the atmosphere-relative velocity vector. Entry conditions for SPORE may vary dramatically, as discussed in Section V, however, the general EDL sequence of events is as follows. Atmospheric entry is defined to occur at a radius of 6,503 km (altitude of 125 km). Peak heating and maximum deceleration are experienced during the hypersonic regime, where the TPS will be exposed to its desired aerothermal environment. The cross parachute is deployed following transition to subsonic flight. No jettison of the heatshield is required, as the payload is thermally isolated from the heatshield soak-back. The vehicle approaches terminal velocity on the parachute prior to touchdown; touchdown velocities vary based upon the vehicle configuration. A UHF beacon signal will be transmitted throughout EDL to aid in the recovery process. Recovery is required to occur within two hours of touchdown. Figure 1 details the baseline EDL sequence of events for SPORE.

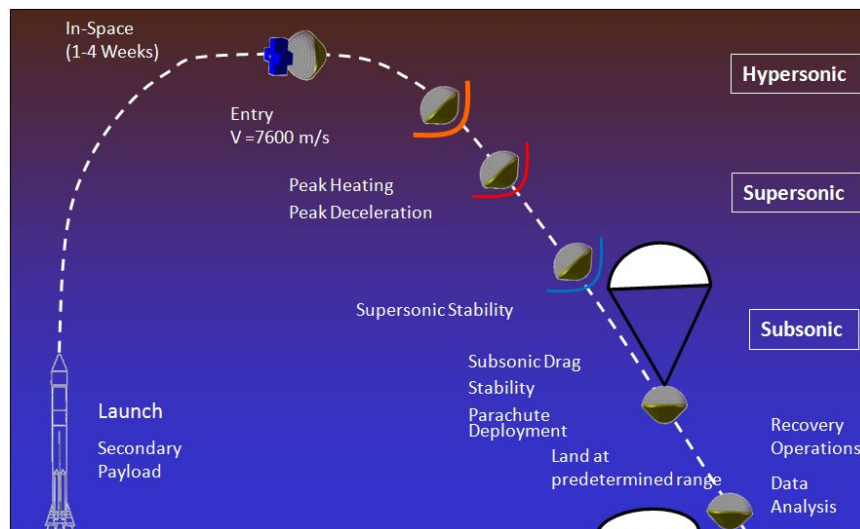


Figure 1. SPORE EDL sequence of events.

III. Driving Requirements: TPS Testbed Mission

In converging on an entry system design and overall mission design, it is important to define and verify the driving requirements. For the SPORE system, a detailed breakdown of all system and subsystem level requirements has been generated. For the TPS testbed mission in particular, there exist several requirements that drive much of the entry system and trajectory design. Many of these flow from payload survival, recovery, and exposure requirements, and are shown in Table 1 below. The landing ellipse constraints were considered in the trajectory Monte Carlo analysis, while the targeted aerothermal environment was considered in the nominal entry trajectory determination, discussed in Section V. Because exposing the TPS to the desired aerothermal environment is key to SPORE mission success, reference Orion ISS and lunar/asteroid return mission environments were used for the maximum stagnation point heat flux and surface pressure requirements. The 5 m/s terminal velocity requirement is set to prevent damage to the TPS upon touchdown, and was used in selecting the Pioneer cross parachute discussed in Section VI. In order to ensure TPS data recovery, such as thermocouple and recession sensor data, the data storage devices and their accompanying electronics boxes must be maintain below their maximum allowable operational temperature (50° C, selected from similar electronics specifications). As a result, a thermal soak-back analysis was performed with FIAT to ensure that this constraint was not violated, and is discussed in Section VII. Finally, the requirement for passive stability and maximum angle of attack stem from the need to have the TPS forward-facing during the hypersonic and supersonic segments of the trajectory, as well as the need to deploy the parachute at a low angle of attack and with the vehicle forward-facing. This is discussed in Section VIII, which covers the re-entry stability analysis using POST.

Table 1. SPORE TPS testbed driving requirements.

Requirement	Driven By:
The SPORE entry system shall be designed so as to enable a landing ellipse no larger than 100 km x 100 km.	Woomera & UTTR Dimensions
The entry system shall be capable of decelerating to a terminal velocity of 5 m/s upon touchdown.	TPS Recovery: Structural Integrity
Sensor data storage devices must be maintained at or below survivable/operational temperatures, 50° C.	TPS Data Recovery
The entry vehicle shall be passively stable through all atmospheric flight regimes, with a 5° maximum angle of attack.	Parachute Deployment & TPS Exposure
During re-entry, the thermal protection system shall be exposed to heat fluxes between 100 and 400 W/cm ² at the stagnation point on the forebody.	LEO Return: Match Orion ISS Return
During re-entry, the thermal protection system shall be exposed to heat fluxes between 500 and 1000 W/cm ² at the stagnation point on the forebody.	GTO Return: Match Orion Lunar/Asteriod Return
During re-entry, the thermal protection system shall be exposed to stagnation pressures between 10 and 25 kPa.	LEO Return: Match Orion ISS Return
During re-entry, the thermal protection system shall be exposed to stagnation pressures between 15 and 50 kPa.	GTO Return: Match Orion Lunar/Asteriod Return

IV. Entry Vehicle Geometry and Packaging

The SPORE TPS testbed flight system architecture is designed to provide access to on-orbit environments and Earth return from LEO and GTO. The flight system consists of a service module, which provides on-orbit functionality and de-orbit capability, and the entry vehicle, which separates from the service module and re-enters the atmosphere. SPORE utilizes the aeroshell geometry developed for the Deep Space-2 Mars Microprobes; the vehicle has a 45° sphere-cone forebody and a hemispherical backshell. Nose radius is $0.25 * D_{max}$, and shoulder radius is $0.1 * D_{max}$, where D_{max} is the maximum diameter of the entry vehicle. The hemispherical backshell has a radius of $0.523 * D_{max}$.

The 1U payload will be used primarily for thermal protection system (TPS) flight experiments, and is designed to accommodate full-scale testing in the NASA Ames Research Center arcjet facilities, necessitating a 40.64 cm (16 in) maximum aeroshell diameter. The current TPS testbed packaging model has a max diameter of 36.26 cm, allowing for TPS thickness growth, as is highly likely. PICA was chosen as the forebody TPS material, because of

its need for characterization at off-nominal heat fluxes (making it a good candidate for TPS testbed missions). A thickness of 0.03175 m was assumed and will be updated once higher fidelity TPS sizing tools are made available. LI900, with a thickness of 0.018 m, was selected as the aftbody TPS, because of its performance as a low-density insulator. For the forebody and aftbody aeroshell structure material, Al-6061-T6 was selected because of its low density, structural integrity, and spaceflight heritage. A thickness of 0.003175 m was assumed and will be updated upon completion of higher fidelity structural analysis.

For the 1U case, the supporting subsystem components are mounted to an Aluminum 6061-T6 central shelf with a central hole for the parachute canister and mortar. The subsystems consist of 3 Saft LSH14 batteries in a battery box, an Aero-Astro communications transceiver in its aluminum shielding, a Space Quest ANT-100 UHF antenna, CubeSat Kit 710-00484 Motherboard and Pluggable Processor Module D1 in their aluminum housing, a power distribution board, and a TPS data processing and storage with an allotted volume: 0.033 x 0.104 x 0.098 m. The main chute is the Pioneer cross parachute, discussed in Section VI. Figure 2 shows the current packaging arrangement for the 1U TPS testbed mission.

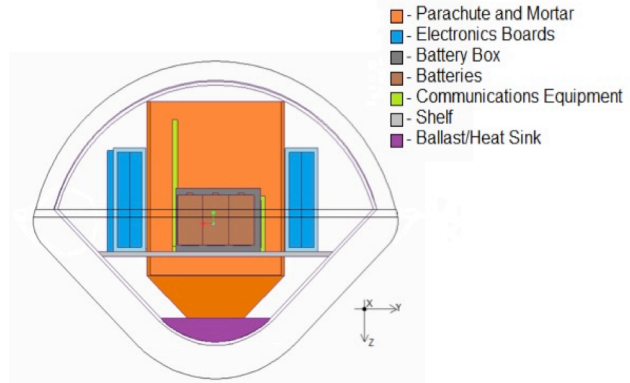


Figure 2. SPORE TPS testbed packaging model.

V. Reference Entry Conditions and Trajectory Design

Reference entry conditions are defined for Earth return from each of the reference orbits (LEO, ISS, GTO), and are dependent upon the entry vehicle mass and geometry based upon payload sizing (1U, 2U, 4U). LEO and ISS-return trajectories will target the Utah Test and Training Range, while GTO-return trajectories are targeted to the Woomera Test Range. The reference entry trajectories for SPORE are shown in Table 2 below.

Table 2. Reference LEO and GTO trajectories.

	LEO	GTO
Longitude (°E)	137.65	127.98
Latitude (°N)	-16.65	-36.4
Velocity (m/s)	7780	9964.4
Flight path angle (°)	-5	-6.71
Azimuth (°)	182.9	57.8
Heading (°)	267.1	32.2

A. Entry State Uncertainty Characterization

The deorbit burn will be performed by a constant thrust, 63 N thruster on the service module. All three orbits—LEO, ISS, and GTO—will follow a nominal trajectory using a trajectory tracking PD guidance controller. Currently, the nominal trajectory is built by applying thrust in the opposite direction of the vehicle’s velocity until the desired amount of delta-V has been attained; however, in the future, the nominal trajectory will be constructed with some type of optimization in mind. After the completion of the burn, the attitude control system (ACS) on the service module will orient the vehicle for reentry. Shortly before reentry, the service module will separate from the entry vehicle. The goal is to characterize the vehicle’s state uncertainty at reentry due to errors in the ACS, guidance system, and GPS. The two main sources of error contributing to the guidance system that are modeled here are the ACS (which controls the orientation of the thrust vector) and the GPS.

For an orbit maneuver, a good estimate for ACS accuracy is a 1° pointing error. To see how this pointing error affects the guidance system error, a MATLAB program was written that simulates an attitude controller operating within a larger guidance control loop. The control law used here is a PD controller that aligns a designated vehicle axis with some vector in vehicle coordinates. To apply this approach to trajectory tracking, the control law aligns the vehicle’s thruster axis with the desired thrust direction supplied by the guidance system. The ACS runs at 10 Hz

while the guidance system operates at 1 Hz, and within each guidance time step, the attitude controller is keeping the thrust vector in proper orientation. The simulation decouples the rotational dynamics from the translational dynamics: for the duration of the outer guidance loop, the attitude portion runs a 3 DOF simulation and saves the resulting thrust vector with error to be applied over that guidance time step. Decoupling the rotational and translational dynamics allows for easy application of the random attitude errors and produces an ACS pointing accuracy of 1°. Figure 3 shows the simulation's block diagram.

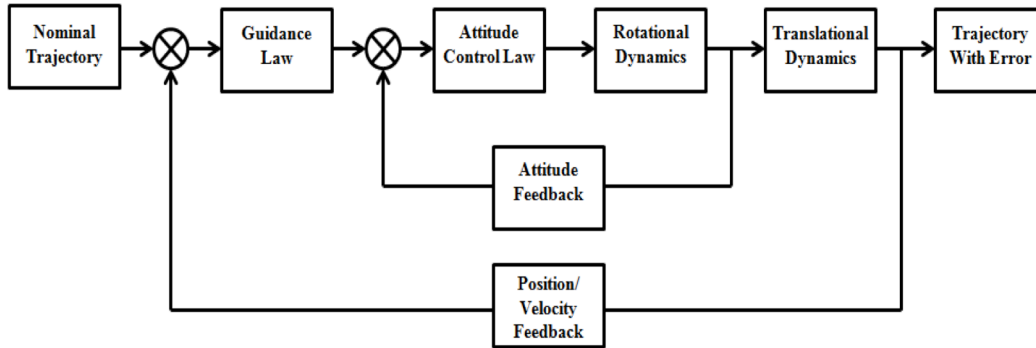


Figure 3. Block diagram of the guidance system simulation.

Since the rotational dynamics are decoupled from the translational dynamics, the simulation is not a 6 DOF, but is a 3+3 DOF simulation.

The other source of error added into the simulation was GPS position and velocity error. The uncertainties used for this analysis are taken from a GPS receiver in use on other small satellites. The position error is 1.8 m, and the velocity error is 0.03 m/s. Now that random errors in the guidance system have been characterized, a Monte Carlo analysis can be wrapped around the simulation to obtain uncertainties at the point of reentry due to the guidance system. For each reference orbit, a 1000 run Monte Carlo was performed and the result 3- σ uncertainties are displayed in Table 3.

Table 3. Re-entry state 3- σ uncertainties.

	LEO	GTO
Flight Path Angle (deg)	0.0053	0.0111
Velocity (m/s)	0.3393	0.0032
Heading (deg)	0.0181	0.004
Latitude (deg)	0.2401	0.0235
Longitude (deg)	0.1663	0.0121

B. Entry Trajectory Simulation

Entry state, aerodynamic, and atmospheric uncertainties were all modeled in the entry trajectory simulations. Entry state uncertainties flow down from the deorbit burn simulation and the 3- σ values listed in Table 3. Since the drag performance of a 45° spherecone has not been accurately characterized in the hypersonic and supersonic regimes, the 3- σ in uncertainties in the aerodynamic database are 0.03 and 0.1 for Mach numbers greater than 10 and less than 5, respectively. Atmospheric uncertainties were modeled by using EarthGRAM (Global Reference Atmospheric Model) to randomly generate tables of 1000 atmospheres. These atmospheres were used in a Monte Carlo simulation and represent the uncertainties in density, temperature, and winds from 0 to 125 km altitude.

A 3 DOF entry trajectory simulation with bank angle modulation was written in MATLAB and served as the primary means of evaluating the entry, descent, and landing trajectory for SPORE. The Sutton-Graves relationship was used for stagnation point heating, and peak decelerations were

Table 4. Trajectory Monte Carlo Summary

	LEO	GTO
Nominal Entry Velocity (m/s)	7,780	9,964
Nominal Entry FPA (°)	-5.00	-6.71
Worst Case Heat Flux (W/cm²)	267.2	514.8
Worst Case Heat Load (J/cm²)	12,857	22,227
Maximum G's	15.65	20.33
Landing Ellipse Downrange (km)	58.50	37.35
Landing Ellipse Crossrange (km)	33.47	4.89

determined to make sure that payload loading requirements were not violated. Currently, parachute deployment is modeled as occurring at an altitude of 5 km, but in the future will be modeled as a G-switch. A deployment altitude of 5 km was chosen as it falls between the 3.1 km main deployment altitude of Stardust and 10 km main deployment altitude of the Hayabusa spacecraft. At this altitude, the entry vehicle is traveling at a low subsonic speed at a near 90° flight path angle.

In the parachute portion of the trajectory, two types of inflation were modeled. For the Monte Carlo simulations, an instantaneous inflation was modeled to save on run time. For the nominal simulations, a linear inflation profile was assumed using Knacke's³ inflation time relationship. This inflation profile, combined with a time delay for line stretch, allowed for re-contact analysis to be performed, ensuring that any deployed fragments of the backshell would not intersect the entry vehicle trajectory. Atmospheric wind contributions to the entry vehicle landing dispersions were modeled, assuming the parachute-vehicle system trimmed to the relative wind vector. Logic was also present in the code to ensure that the maximum dynamic pressure parachute constraints were not violated. 250 Monte Carlo cases were run in order to capture the extremities of the landing ellipse while keeping run time short for the rapid iteration design process. The results for the 1U LEO and GTO Case are shown in Figure 4 and Table 4.

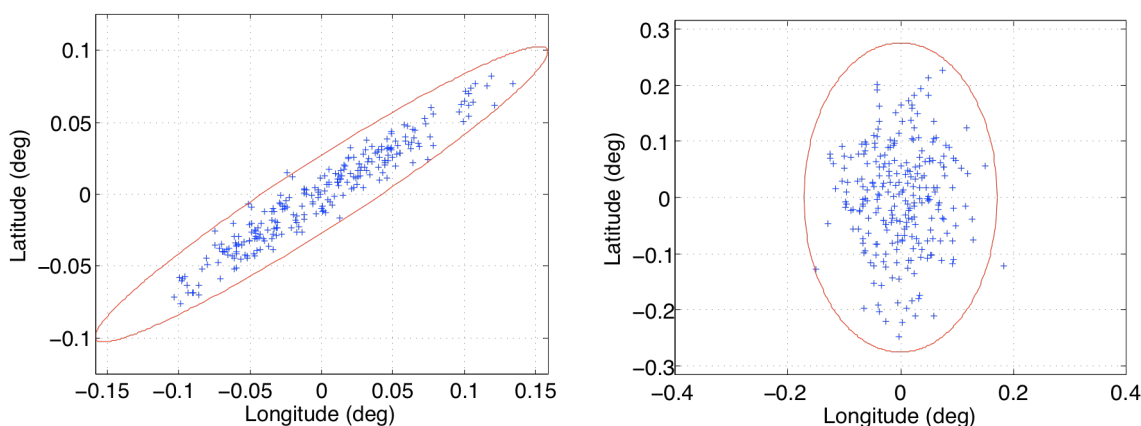


Figure 4. Landing Ellipse with Monte Carlo data for (a) LEO and (b) GTO.

VI. Parachute Selection and Deployment

In order to keep the payload intact upon impact with the ground, the vehicle's parachute must keep the impact speed below 5 m/s. The 1U vehicle will use a cross parachute manufactured by Pioneer Aerospace for use on 16 kg flares. The parachute is capable of meeting the 5 m/s requirement for vehicles less than 18 kg. A mortar for this parachute consists of a gas generator with electrical ignition, which will push up a sabot and eject the packaged parachute from the top of the backshell. A backshell cap, held in place by shear pins, will pop off when pressure becomes too great and release the parachute.

To avoid supersonic and transonic instabilities, it was decided that the parachute shall be deployed subsonically, at Mach 0.8. From preliminary simulation data this occurs at an altitude in between 20 to 30 km, depending on the entry vehicle configuration. A gravity switch (G-switch) will be utilized to initiate backshell jettison at the desired deceleration level during atmospheric entry. Using Monte-Carlo trajectory simulations, the relationship between deceleration profiles and dynamic pressure will be characterized across the expected flight regime. A target deceleration will be established based upon the backshell aerodynamics and parachute inflation loads. Historically, a 3-G trigger (on the downslope of the entry deceleration curve) has been used for parachute deployment of the Stardust and Genesis missions. When the G limit is obtained, the trigger circuit is armed and fires the deployment device after the predetermined time. As a backup to the G-switch based parachute deployment, a target change in time (Δt) relative to the atmospheric interface point may be used to initiate drogue cap separation and parachute deployment. This straightforward approach has been used for the Mars Pathfinder, Mars Exploration Rover, and the Phoenix Mars Lander missions. The targeted time from atmospheric interface is used as a default time for initiating backshell separation, and is biased late to allow the primary G-switch deployment mode to trigger deployment; this default time is overwritten in flight software parameter tables when the G-switch based deployment time is

established. The current Monte Carlo analysis was performed assuming an altitude trigger, but will be updated later to include a G-switch (See Section VI).

VII. Thermal Soak-back Analysis

In order to verify that the electronics boxes do not exceed their maximum allowable operational temperature during re-entry, a thermal soak-back analysis was performed using FIAT (Fully Implicit Ablation and Thermal Response) program. For this analysis, the worst-case heating trajectories from the Monte Carlo simulation mentioned in Section V were used. The stagnation point convective heating was approximating using the Sutton-Graves relationship, while the radiative heating was approximated using the Martin relationship for Earth entry. The “assigned surface temperature history” option was used in FIAT for the re-entry segment, while the “cool-down” option was used for a 10,000 second cool down period. The surface temperature was approximated assuming that the re-radiated heat flux is equivalent to the convective and radiative heating, as shown in Equation 1.

$$T_{surf} = \left(\frac{q_{rerad}}{\epsilon\sigma} \right)^{1/4} \approx \left(\frac{q_{conv} + q_{rad}}{\epsilon\sigma} \right)^{1/4} \quad (1)$$

The surface pressures were estimated using normal shock relationships at the vehicle nose, using the freestream density and vehicle Mach number. A plot of the total stagnation point heat flux for the worst case heating trajectories, along with the calculated surface temperatures and pressures are shown in Figure 5 below. As one can see, the worst case surface temperatures correspond to the GTO return trajectory with the worst case heat flux. Therefore, this assigned temperature and pressure profile were used for the 1-D FIAT heat soak back analysis and heat sink thickness optimization.

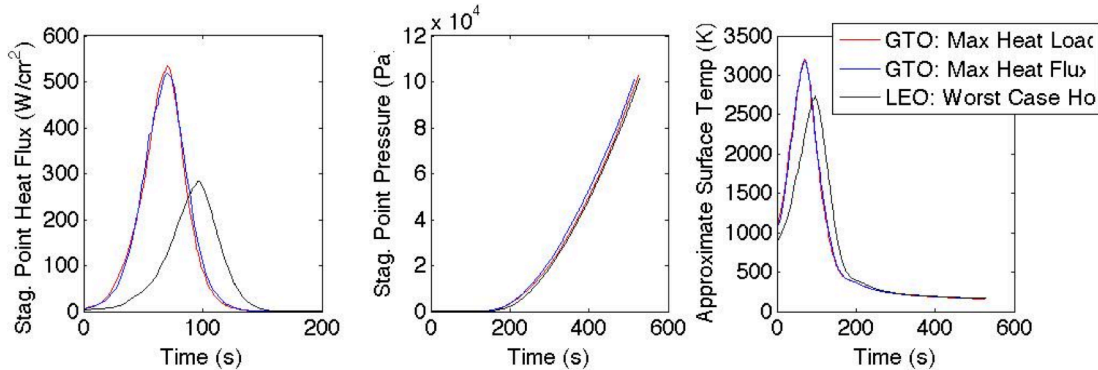


Figure 5. Worst case heating trajectories: (a) total stagnation point heat flux, (b) surface pressure, and (c) surface temperature.

The material stack-up used is that described in Section IV: PICA, RTV-560V, Al-6061 forebody structure, Al-6061 heat sink material, radiative gap (air), and the electronics boxes (Al-6061). For the worst case heating trajectory from GTO, the optimized heat sink thickness was determined to be 41.2 mm. The temperature profiles at the base of each of the layers in the material stack-up are shown in Figure 6. As one can see the base of the electronics boxes is maintained below the 50°C constraint.

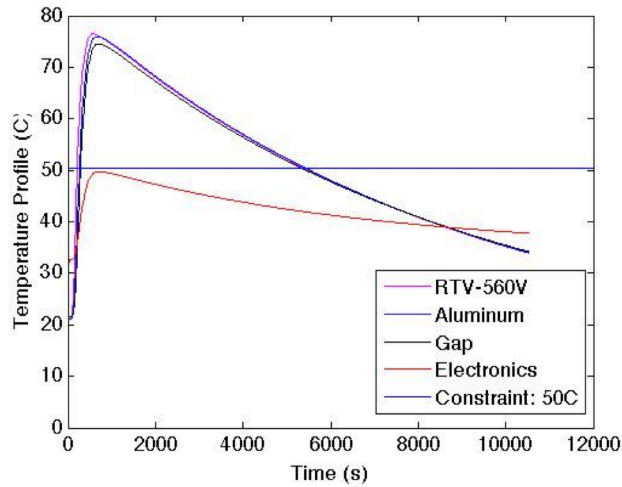


Figure 6. Temperature profiles for the worst case heating trajectory.

VIII. Stability During Re-entry

SPORE adopted the Mars Microprobe axis-symmetric, 45-degree spherecone geometry to be passively stable during all phases of atmospheric entry.³ Research completed at NASA Langley estimated the center of gravity should be located at 34.6% of the diameter along the centerline of the vehicle to achieve passive stability.⁷ Due to packaging constraints, this center of gravity requirement cannot be met for the 1U TPS vehicle. As a result, a 6DOF model of the SPORE entry trajectory was created using POSTII to assess dynamic stability during the hypersonic, supersonic, transonic, and subsonic Mach regimes.

The 6 DOF model uses the Mars Microprobe aerodynamic database found in literature³ and 1976 standard atmospheric tables. To simulate a passive entry vehicle, no steering was applied to the model and the vehicle was initialized for ballistic entry. The model does not include a parachute so that dynamic stability can be assessed throughout the entire trajectory. Atmospheric winds were not included in this model.

The 6 DOF model was run for the nominal LEO trajectory. The vehicle is considered dynamically stable if the total angle of attack remains under five degrees.¹ Results show that the entry vehicle remains stable throughout the entire entry trajectory. There is a slight increase in total angle of attack as the vehicle approaches the transonic regime, but the oscillations remain well within the stability requirement and damp out over time. The model has the option to spin the vehicle to increase dynamic stability, but results show this is not necessary. The total angle of attack versus Mach number and time is plotted in Figure 7.

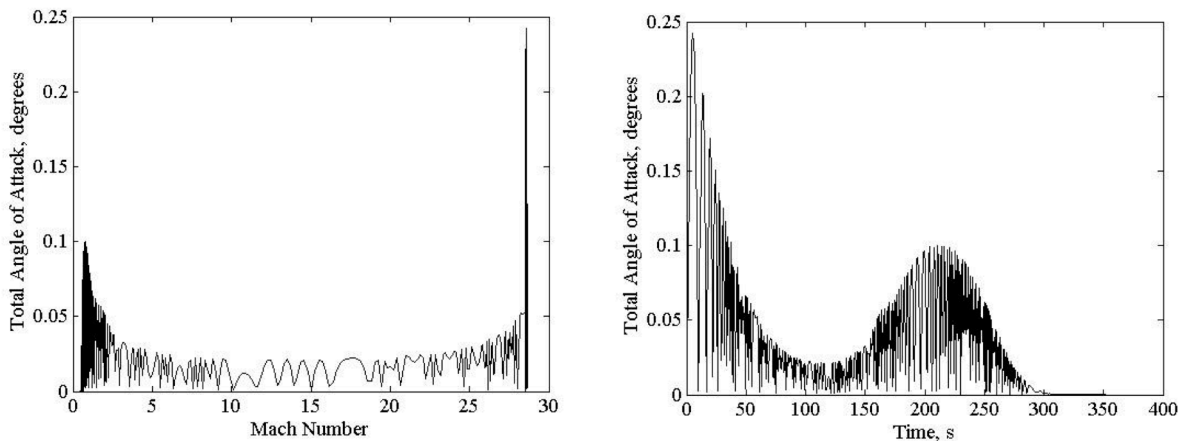


Figure 7. (a) Total angle of attack vs. Mach number. (b) Total angle of attack vs. time

IX. Mass Budget

The mass budget for the SPORE entry vehicle is shown in Table 5, based upon the TPS testbed configuration. A description of the various components within the packaging model can be found in Section IV. The parachute mass and mortar mass were estimated assuming a packaging density of 640 kg/m³ and a chute area of 9.08 m² and using relationships found in Knacke³ and Pawlikowski et al.⁶ For mass margins, if the item was sized using similar historical missions and not using direct analysis, it was given a 15% margin. If the component was sized using first-order analysis, it was given a 10% margin; if the analysis was conservative, it was given a 5% margin. Finally, if the mass of the component is directly known, it was given zero margin.

Table 5. Entry vehicle mass budget

	Initial Estimated Mass (kg)	Margin (%)
Forebody Structure	0.96	15
Aftbody Structure	1.08	15
Forebody TPS	1.20	5
Aftbody TPS	0.40	15
Payload (TPS Data Storage Unit)	0.52	0
Component Shelf	0.54	10
Primary Batteries (3)	0.26	10
Power Control Board/ Battery Mounting	0.45	10
Processor & Avionics	0.65	10
Antennae	0.22	10
Communications Transmitter	0.31	10
Parachute & Canister	1.44	15
Mortar	1.47	10
Heatsink	1.01	15
Total Entry Vehicle Mass (kg):	10.51	

X. Conclusions

The conceptual design for the SPORE entry, descent and landing system has resulted in a simple, low-cost system that provides the capability to return small payloads to Earth from a broad range of potential orbits. The above paper summarizes the current design of the TPS testbed mission, which seeks to provide LEO and GTO Earth-return aerothermal environments for TPS characterization. Key design attributes include an aerodynamically stable entry geometry, a subsonic cross parachute, and a UHF beacon to assist in recovery operations. Through this conceptual design process, the feasibility of a standardized platform for re-entry and recovery of small payloads has been established for a TPS flight test platform for direct comparison to Arcjet facility test data.

Acknowledgments

The work described in this paper was conducted by Aurora Flight Sciences Corporation and the Georgia Institute of Technology under the NASA Small Business Technology Transfer (STTR) program.

References

- ¹ D. A. Spencer and R. D. Braun, "Mars Pathfinder Atmospheric Entry: Trajectory Design and Dispersion Analysis", *Journal of Spacecraft & Rockets*, Vol. 33, No. 5, Sept-Oct. 1996, pp. 670-676.
- ² Hinada, Motoki, et. al., "Parachute System of MUSES-C Reentry Capsule," *CEAS/AIAA Aerodynamic Decelerator Systems Technology Conference, 15th*, Toulouse, France, 8-11 June 1999, Collection of Technical Papers (A99-30926 07-03).
- ³ Knacke, T. W. *Parachute Recovery Systems Design Manual*. 1st ed. Para Publications: Jan 1992.
- ⁴ Mitcheltree, R.A., Moss, J.N., Cheatwood, F.M., Greene, F.A., and Braun, R.D., "Aerodynamics of the Mars Microprobe Entry Vehicles," AIAA Paper 97-3658, *Atmospheric Flight Mechanics Conference*, New Orleans, LA, August 11-13, 1997.
- ⁵ Otero, R.E. and Braun, R.D., "The Planetary Entry Systems Synthesis Tool: A Conceptual Design and Analysis Tool for EDL Systems," *IEEE Aerospace Conference Proceedings*, Paper No. 1331, Big Sky, MT, March 2010
- ⁶ Pawlikowski, T.P. "Drogue Mortar System Development and Performance Evaluations." *AIAA Journal*, AIAA 2490-977, 1986 pp. 318-326.
- ⁷ R. A. Mitcheltree, C. M. Fremaux, and L. A. Yates, "Subsonic Static and Dynamic Aerodynamics of Blunt Entry Vehicles," AIAA 99-1020, *37th Aerospace Sciences Meeting and Exhibit*, Reno, NV, Jan. 1999.